STRUCTURAL EFFICIENCY VIA MINIMISATION OF ELASTIC ENERGY IN DAMAGE TOLERANT LAMINATES

M. Nielsen[a], A. T. Rhead[a], R. Butler[a*]

[a]*Department of Mechanical Engineering, University of Bath, Bath, UK*
**R.Butler@bath.ac.uk*

Keywords: Elastic energy, optimization, damage tolerance, minimum mass.

Abstract
Genetic Algorithm and exhaustive search techniques identify balanced symmetric stacking sequences that minimise elastic energy to produce optimal structural efficiency under combined loading. Constraints are added to account for use of standard ply angles, laminate design rules and damage tolerance. The damage tolerant strength constraint produces a bi-level optimization problem: surface plies are orientated to sufficiently minimise energy available for sublaminate buckling driven delamination propagation; core plies are orientated to maximise stiffness in response to a uniaxial load case. The proposed methodology demonstrates that current, standard ply angle, aerospace designs can be near optimal for undamaged strength. However, continuous angles and relaxation of design rules offer significant scope for improved damage tolerance.

1. Introduction

Verchery [1] has shown that Netting analysis, in which the fibres within a laminate are aligned in principal directions to carry principal stresses, can be treated as a limiting case of Classical Laminate Theory. His approach indicates that designs with fewer than three fibre directions produce mechanisms when subject to small disturbances in loading. For example, fibres within a cross-ply laminate, Fig.1 (a), cannot sustain shear load; Netting analysis reveals that this laminate becomes a mechanism when subject to shear because the associated compliance matrix is singular. By similar reasoning, angle-ply laminates, Fig. 1 (b), cannot support bi-axial load. These concepts reveal the reasoning behind established laminate design practice in which fibres are placed in four principal directions (0°, +45°, -45° and 90°). Such laminates provide a level of redundancy in load carrying whilst allowing for the manufacturing requirement of balanced angle plies, Fig. 1 (c).

However, Netting analysis leads to laminate designs in which the stresses in fibres are limited to some value associated with failure, i.e., fully-stressed fibre design. It ignores the effect of damage in the resin matrix, which may occur within (intra) or between (inter) plies. It also assumes pristine material properties and ignores the influence of damaging events such as impact. Since it is well known that in compressively-loaded laminates, the effect of delamination damage can reduce strength by over 60%, consideration of such damage during laminate design is of critical importance. In this paper, we aim to incorporate the fully stressed (Netting) design principle whilst allowing for damage by simultaneously (i) minimizing the elastic energy within the laminate for a given loading and (ii) meeting the required damage tolerant strength of the laminate.

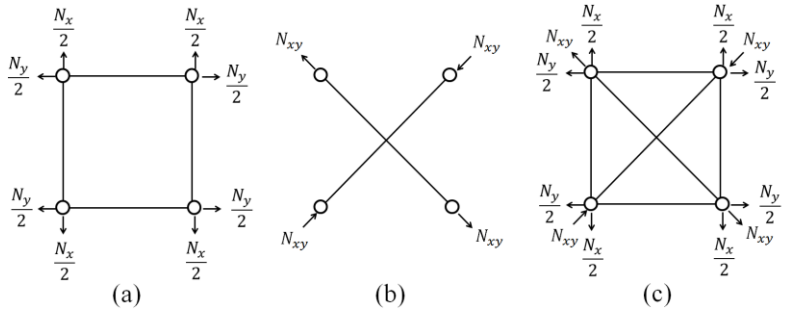

Figure. 1 Netting analysis principles applied to (a) cross-ply laminate carrying bi-axial load N_x and N_y (b) angle-ply laminate carrying shear load N_{xy} and (c) 0°, +45°, -45° and 90° laminate carrying general loads N_x, N_y and N_{xy}. In each case, the simple truss can be used to represent the loading of fibres.

2. Netting Analysis and Minimisation of Elastic Energy

Genetic Algorithm (GA) and exhaustive search techniques are used to find the fibre angle distribution that most efficiently carries a combined (axial, transverse, shear) loading whilst satisfying laminate design rules and Damage Tolerance (DT) constraints. The structural efficiency of a given volume of fibrous layers is assumed to be given by its Hookean Strain Energy as is explained in the following.

Assuming symmetric, balanced laminates (ie. **B** = 0 and A_{13}, A_{23} = 0) and a state of plane stress ($\sigma_z, \tau_{xz}, \tau_{yz} = 0$), classical laminate theory gives the in-plane load-strain relationship as

$$\boldsymbol{N} = \begin{Bmatrix} N_x \\ N_y \\ N_{xy} \end{Bmatrix}_L = \boldsymbol{A\varepsilon} = \begin{bmatrix} A_{11} & A_{12} & 0 \\ A_{12} & A_{22} & 0 \\ 0 & 0 & A_{33} \end{bmatrix}_L \begin{Bmatrix} \varepsilon_x \\ \varepsilon_y \\ \varepsilon_{xy} \end{Bmatrix}_L \tag{1}$$

where N_x, N_y, N_{xy} and ε_x, ε_y, ε_{xy} are the in-plane axial, transverse and shear loads per unit width and corresponding laminate strains, respectively. The A_{ij} terms represent the in-plane stiffnesses and subscript 'L' denotes laminate as opposed to sublaminate variables.

The elastic energy for a linear elastic solid is given by

$$U = \frac{1}{2}\int \boldsymbol{\sigma}^T \boldsymbol{\varepsilon}\, dV \tag{2}$$

Then from Eq. (1)

$$U = \frac{1}{2}\int \boldsymbol{\sigma}^T \boldsymbol{A}^{-1}\boldsymbol{N}\, dV \tag{3}$$

Constant ply thickness is assumed in order that a DT strength constraint can be applied during optimisation. Working per unit width allows for laminate plate geometry to be ignored and for strain energy per unit area to be used to observe the effect of fibre angle distribution on laminate elastic energy. Hence given that $\boldsymbol{\sigma} = \boldsymbol{N}/T_L$ (T_L is laminate thickness) and $dV = T_L dA$,

$$U = \frac{1}{2}\int \boldsymbol{N}^T \boldsymbol{A}^{-1}\boldsymbol{N}\, dA \tag{4}$$

and thus the elastic energy per unit area is

$$U_A = \frac{1}{2}\,\boldsymbol{N}^T \boldsymbol{A}^{-1}\boldsymbol{N} = \frac{1}{2}\left(a_{11}N_x^2 + 2a_{12}N_xN_y + a_{22}N_y^2 + a_{33}N_{xy}^2\right) \tag{5}$$

Netting analysis assumptions remove the coupled compliance a_{12} in Eq. (5) and give

$$a_{11} = \frac{1}{E_{11}t_0},\ a_{22} = \frac{1}{E_{11}t_{90}},\ a_{33} = \frac{1}{E_{11}t_{45}} \tag{6}$$

according to Netting analysis assumptions Fig. 2 shows that when

$$\frac{N_x}{E_{11}t_0} = \frac{N_y}{E_{11}t_{90}} = \frac{N_{xy}}{E_{11}t_{45}} = \varepsilon_{ult}\ , \tag{7}$$

the thickness of layers is optimal (fully stressed). In this case, Eq. (5) gives

$$U_A = \frac{\varepsilon_{ult}}{2}\left(N_x + N_y + N_{xy}\right) \tag{8}$$

where U_A is minimised for the case $\varepsilon_{layers} = \varepsilon_{ult}$. This confirms minimisation of elastic energy in a laminate of fixed thickness maximizes undamaged laminate strength.

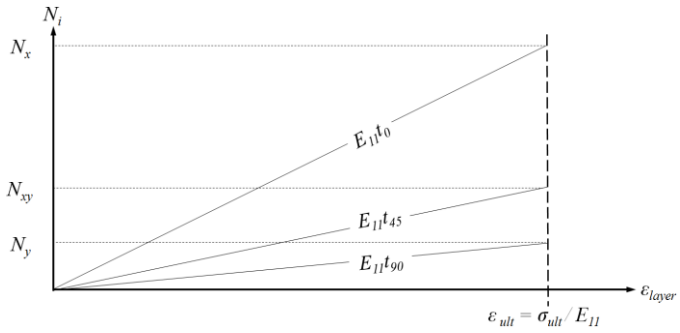

Figure 2. Netting analysis for the fully stressed design of 0º, 45º and 90º laminate layer thicknesses for general loading seen in Fig.1 (c). ε_{ult} is the failure strain of a ply in the direction of fibres.

3. Damage Tolerance Strip Model

The reduction in strength of compressively loaded structures containing multiple, impact-damage-derived delaminations is currently limiting weight reduction in aerospace composite structures. Under compressive loading, layers above such delaminations (sublaminates) can buckle, driving delamination growth (see Fig. 3) and ultimately causing failure. Hence it is necessary to account for this failure mechanism when deriving optimal laminate designs.

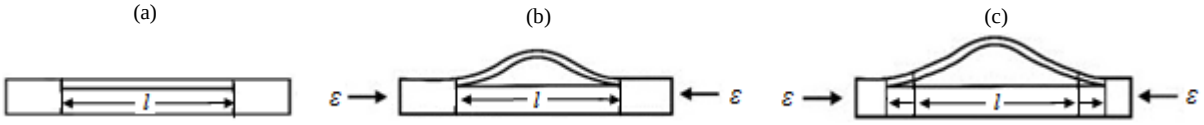

Figure 3. (a) Sublaminate of diameter l created by delamination following an impact. (b) Buckling of sublaminate $\varepsilon \geq \varepsilon^C$ and (c) propagation of delamination $\varepsilon \geq \varepsilon_{th}$. Here ε^C is the sublaminate buckling strain and axial delamination growth in (c) could initially occur laterally once ε equals the threshold strain ε_{th}.

The Strip model [2] is an analytical method based on this sublaminate-buckling-driven delamination propagation mechanism and is used to calculate an axial threshold stress σ_{th} below which delamination propagation will not occur. The strip model compares membrane and bending energy before and after propagation in the post-buckled system described in Figure 3 to calculate a Strain Energy Release Rate (SERR) G_I,

$$G_I = \frac{A}{2}(\varepsilon - \varepsilon^C)(\varepsilon + 3\varepsilon^C) \tag{9}$$

Here A is the sublaminate axial stiffness and is equal to A_{11} if $A_{11} \geq A_{22}$ and A_{22} otherwise, ε^C is the sublaminate axial buckling strain and ε is the applied uniaxial strain. Delamination propagation is assumed to occur when there is sufficient applied strain ε_{th} to make G_I equal to the Mode I fracture toughness of the resin matrix (G_{IC});

$$G_{IC} = \frac{A}{2}(\varepsilon_{th} - \varepsilon^C)(\varepsilon_{th} + 3\varepsilon^C) \tag{10}$$

As the severity of an individual impact is unknown *a priori* and will result in uncertain delamination sizes and depths the worst case (minimum) ε_{th} must be assumed at all interfaces. (The depth of delamination considered to be at risk of propagation is limited to 25% of the laminate thickness as the thicker sublaminates associated with deeper delaminations will not buckle open and allow Mode I propagation to occur [3].) ε^C is the only variable dependent on delamination size in Eqs. (9 and 10). Hence, the uncertainty in damage morphology can be mitigated by finding the minimum value (with respect to ε^C) of ε_{th} in Eq. (10). Implicit differentiation of Eq. (10) with respect to ε^C gives

$$\frac{dG_{IC}}{d\varepsilon^C} = \frac{A}{2}\left[2\varepsilon_{th}\left(\frac{d\varepsilon_{th}}{d\varepsilon^C}\right) + 2\varepsilon^C\left(\frac{d\varepsilon_{th}}{d\varepsilon^C}\right) + 2\varepsilon_{th} - 6\varepsilon^C\right] \tag{11}$$

As $\frac{d\varepsilon_{th}}{d\varepsilon^C} = 0$ is sought and G_{IC} is constant (and thus $\frac{dG_{IC}}{d\varepsilon^C} = 0$) rearrangement of Eq. (11) gives

$$\varepsilon^C = \frac{\varepsilon_{th}}{3} \tag{12}$$

Substitution into Eq. (10) then gives the minimum value of ε_{th} and multiplication by the laminate modulus E_{xx} gives the required minimum threshold stress,

$$\sigma_{th,min} = E_{xx}\sqrt{\frac{3G_{IC}}{2A}} = \frac{1}{T_L}\left(A_{11L} - \frac{A_{12L}^2}{A_{22L}}\right)\sqrt{\frac{3G_{IC}}{2A}} \tag{13}$$

As Eq. (13) is independent of ε^C, minima may correspond to unrealistically large delamination diameters and thus can be a very conservative lower bound on ε_{th} for realistic damage e.g. (BVID). Note that Eq. (12) guarantees that delamination growth will be stable i.e. propagation will only occur with increasing strain (see [4] for full details and derivation). The derivation of Eqs. (9 and 10) includes the following simplifying assumptions: (1) loading is uniaxial and compressive; (2) energy for propagation is only available from the thin sublaminate (thin-film assumption); (3) Mode I fracture dominates propagation; (4) delaminations at each interface and their subsequent propagation under compressive load can be treated in isolation with the lowest of the derived propagation stresses σ_{th} taken as the overall laminate residual strength.

4. Optimisation for Minimum Strain Energy and Damage Tolerance

4.1 Objective function and problem description

The loading on an aerostructural panel is typically dominated by an axial component. However, lateral loading can occur and may induce significant shear and transverse components. As described in Section 2 optimal laminate designs should distribute fibres to meet theses loads thereby producing an efficiently loaded structure. This equates to minimising elastic energy for a given laminate thickness. For both continuous and standard ply angle laminates and subject to the constraints defined below, an exhaustive search technique and the Matlab Genetic Algorithm (GA) function '*ga*' [5] are used to find an optimal fibre angle distribution and stacking sequence through minimisation of U_A in Eq. (5). For a given laminate thickness, subject to in-plane loading per unit width ($\boldsymbol{N}$), the GA creates an initial random population of candidate stacking sequences and then calculates a scored fitness value for each. The most energy efficient designs are chosen and used to determine the next generation/population of stacking sequences. (Eliteness, crossover and mutation all feature in *ga*.) A nonlinear constraint algorithm is employed to ensure that each new generation of stacking sequences meets a set of constraints derived in Section 4.2. Iteration

continues until a maximum number of generations or specified minimum relative change in best fitness value is reached.

4.2 Laminate design and damage tolerance constraints

Aerospace laminates are subject to certain manufacturing and design constraints. *Zero in-plane to out-of-plane coupling* is enforced for standard angle laminates by allowing free choice of ply angles in one half of the laminate only. For continuous ply angle laminates it is achieved via use of the fully uncoupled Winckler [6] ply block [θ/-θ/θ/θ/-θ/θ/θ/-θ] (henceforth defined as $(\theta)_W$) and symmetry in α (Fig. 4). *Balance* of standard ply angle laminates is enforced by the constraint $A_{13L} = A_{23L} = 0$. For continuous ply angles, balance is again achieved via Winckler sequences. When *laminate design rules* [7] are applied: (1) *maximum ply grouping* is constrained to be less than 4 plies of the same orientation. This prevents the formation of large inter-laminar shear stresses that may drive free edge failure. In the continuous angle laminates, ply groups are assumed to be sufficiently separated by an angular separation of ±12.5° (see Fig. 4). (2) *minimum ply percentages* of 10% of each of 0º, ±45º and 90º ply angles safeguard against uncertainty in loading. *Damage Tolerance* (DT) is ensured by allowing the GA to accept a stacking sequence as a candidate only if σ_{th} exceeds a minimum stress constraint determined by Eq.(13).

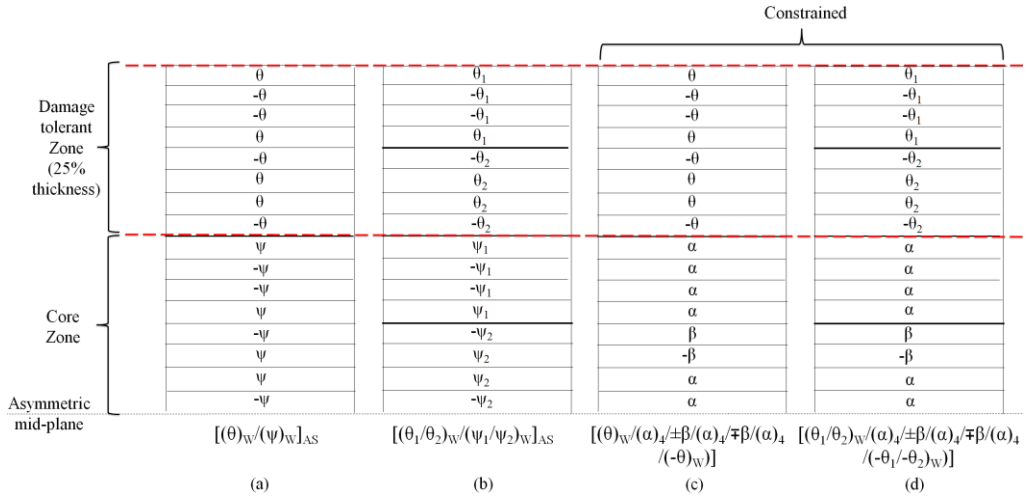

Figure 4. Details of candidate stacking sequences for optimisation (a) two and (b) four variable continuous ply angles without constraint. (c) and (d) alternative stacking sequences available when laminate design rule constraints are active. The DT constraint (where applied) affects the outer 25% of layers.

5. Results

Stacking sequences with two, three and four continuous ply angles (see Fig. 4) are compared to laminates with standard ply angles; the maximum structural efficiency available while employing current laminate design rules is determined and scope for improvement highlighted. Material properties E_{11} = 145 GPa, E_{22} = 8.9 GPa, G_{12} = 4.2 GPa, ν_{12} = 0.35, G_{IC} = 500 J/m^2 and ply thickness = 0.125 mm are assumed. Elastic energy, normalised by the sum of the squares of the load components (after Eq. 5), is used to compare the structural efficiency of stacking sequences for varied combined loadings;

$$\bar{U} = \frac{U_A}{(N_x^2+N_y^2+N_{xy}^2)} \tag{14}$$

For variable loading ratios (and both with and without laminate design rules) Figs. 5(a) and (b) show the variation of minimum normalised elastic energy (structural efficiency) of

laminates optimised using either continuous or standard ply angles. Figures 5(c) and (d) show standard angle ply percentage variation for varying ratios of axial to transverse and shear loading, related to the curves of Figures 5(a) and (b). For the major part of the continuous ply curves in Fig. 5(a) and (b) stacking sequences described by Fig. 4(a) and (b) are sufficient to produce minimum $\bar{U}$. However, when one load component and hence one fibre orientation dominates, stacking sequences from Fig. 4 (c) and (d) become optimal.

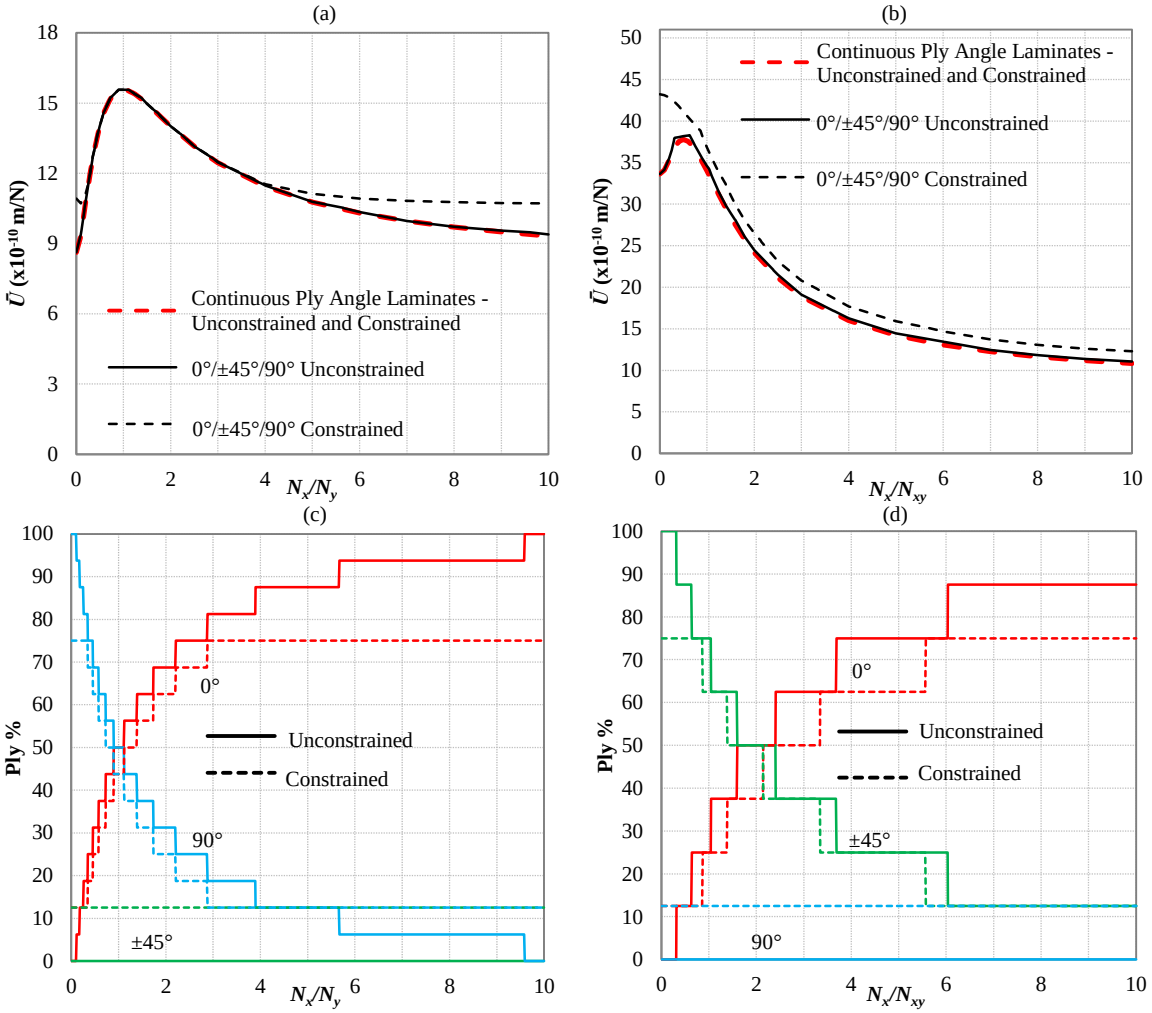

Figure 5. Normalised elastic energy $\bar{U}$ of optimal laminates with continuous and standard ply angles for varying loading ratio (a) N_x/N_y and (b) N_x/N_{xy}. Standard laminate ply percentages for varying loading ratio (c) N_x/N_y and (d) N_x/N_{xy}. Curves are shown for constrained (with laminate design rules) and unconstrained (without) cases.

Figure 6(a) compares the elastic energy of optimum stacking sequences of continuous (see Fig. 4) and standard ply angles for uniaxial compression ($N_y = N_{xy} = 0$) subject to a minimum DT strength constraint. The stacking sequences relating to peak DT stress for standard ply angle laminates are $[\pm 45_2/0_2/90_2/0_8]_S$ and $[0_4/90_4/45/0_4/\text{-}45/0_2]_S$ for the unconstrained and constrained cases respectively. Peak DT stresses are 350 MPa and 305 MPa respectively. Figure 6(b) gives the optimum ply angles for continuous laminates corresponding to the curves in Fig. 6(a). The stacking sequences relating to peak DT stress for 4 continuous ply angle laminates are: sequence (b) in Fig. 4 with $\theta_1 = 20°$, $\theta_2 = 70°$, $\psi_1 = \psi_2 = 0°$ and sequence (d) with $\theta_1 = 17°$, $\theta_2 = 73°$, $\alpha = 0°$ and $\beta = 12.5°$. Maximum DT stresses are 350 MPa and 344 MPa respectively.

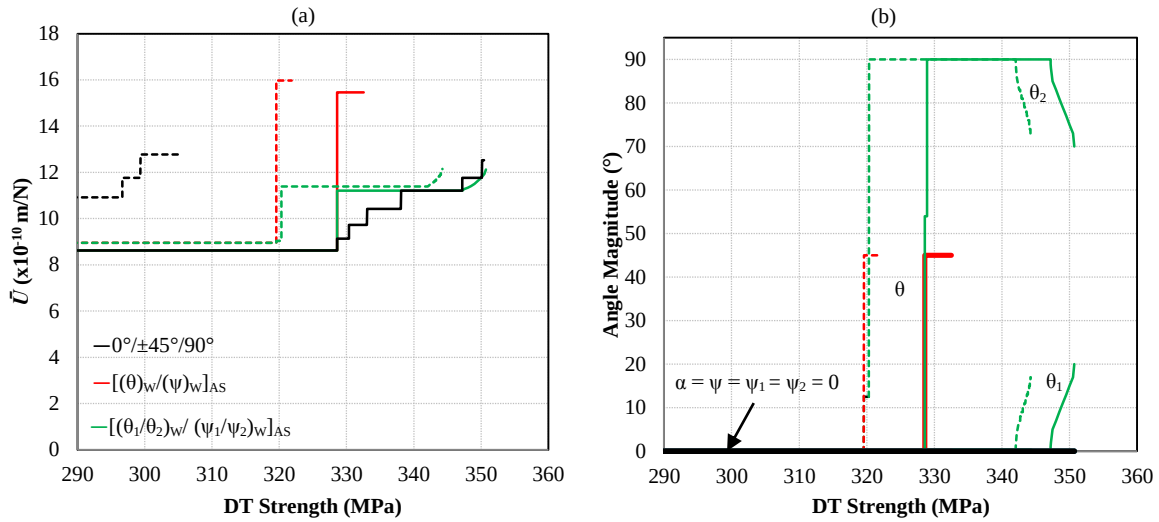

Figure 6. (a) Normalised elastic energy $\bar{U}$ of optimum stacking sequences for constrained (dotted line) and unconstrained (solid line), laminates with increasing minimum damage tolerant strength. (b) Optimum angles for continuous designs in (a). Note that the ungrouping ply angle β is not plotted but is always ±12.5°.

6. Discussion

Under loading with a dominant component (and no DT constraint), Fig. 5 demonstrates that current design rules combined with standard ply angles allow for near maximum efficiency until the minimum ply-percentage rule becomes active. Worst-case structural efficiency occurs for loading ratios of $N_x = N_y$ or $2N_x = N_{xy}$ with the exception that constrained standard ply angle designs are least efficient under pure shear loading (see curve maxima in Figs. 5 (a) and (b)). Hence care should be taken in specifying worst-case design loadings. Figures 5 (c)-(d) illustrate that, as expected, optimal designs have fibres aligned with the applied loading i.e. 0º dominates for high load ratios. It is again evident that the minimum ply percentage constraint prevents full structural efficiency being reached for loadings with dominant axial components. Current ply percentage designs of 44/44/12 and 60/30/10 (percentage of 0º/±45º/90º plies) are only an optimal choice of design when loading has a shear component (contrast Figs. 5 (c) and (d)), e.g. at loading ratios of approximately $N_x/N_{xy} = 2$ and $N_x/N_{xy} = 3$-6 respectively. For other load cases e.g. biaxial loading (Fig. 5(c)) other ply percentages are more efficient. As per Netting analysis in Section 1, although limiting for structural efficiency, the ply percentage constraint is likely to improve resilience to intra-ply failures resulting from formation of mechanisms (Figures 1(a) and (b), [8]) and therefore its implementation is well justified. Results in Fig. 5 are given as ply percentages and so optimum efficiency may have been achieved by a number of unique stacking sequences. Peak unconstrained DT strength (see Fig. 6(a)) is achieved by orientating outer plies at ±70° and ±20° and inner plies at 0°. The former strikes a balance (in Eq. 13) between sufficiently minimising A (sublaminate SERR) and maximising E_{xx} to provide maximum laminate stiffness. The latter gives minimum elastic energy for uniaxial load. From netting analysis the continuous ply design has no redundancy and thus is better optimised but less robust than the standard ply stacking sequence. A maximum DT strength of 350 MPa is reached for both standard and continuous angle plies where no further improvement is possible. However, unconstrained continuous angles offer a slightly higher structural efficiency at maximum DT constraint. When ply grouping constraints are applied, the effect is to reduce the maximum DT strength, see Fig. 6(a). However, the reduction in achievable DT stress is considerably greater for the standard ply designs. It is conjectured that this discrepancy will increase for non-uniaxial loadings as the flexibility of the continuous ply angles will provide scope to more efficiently distribute fibres to the meet the applied loads. Delamination propagation is

currently limited to being stable (Section 2, [4]), a more stringent constraint than is required by regulation. Hence future work will consider unstable growth and any increase in DT strength that may be available.

7. Conclusions And Future Work

Using the principles of Netting analysis and fully stressed design, minimization of elastic energy through stacking sequence optimization has allowed identification of structurally efficient designs for flat plates. Subject to the standard laminate conditions of balance and no in-plane to out-of-plane coupling, two design cases have been considered. The first allows for up to four independent choices of ply orientation and the second restricts ply angle choice to 0º, ±45º and 90º. Both cases are considered with and without constraint by standard laminate design rules. Results indicate that when laminate design rules are applied, standard ply laminates are close to matching the optimal structural efficiency of continuous ply angle designs for bi-axial and axial/shear loading cases without a dominant load component. When a damage tolerance constraint is imposed with pure uni-axial loading and no design rule constraints, both continuous and standard ply angle laminates offer a peak compressive strength of 350 MPa with little difference in structural efficiency. However, when constrained by laminate design rules, continuous ply laminates offer significant improvements in structural efficiency and the peak damage tolerance strength achievable relative to the standard angle design. The optimization and analysis methods implemented here are analytical in nature and thus have the computational efficiency required for early stage design. Future work will focus on: optimizing for an uncertain combined loading; incorporation of in-plane failure and global buckling constraints and combined loading with a damage tolerant constraint.

Acknowledgements

Richard Butler is supported by a Royal Academy of Engineering/GKN Aerospace Research Chair in Composites Analysis. The help of Jonathan Chesterfield, University of Bath, is gratefully acknowledged.

References

[1] G. Verchery. The Netting analysis as a limit case of the laminated structure theory. In *19th International Conference on Composite Materials*, Montreal, Canada, 2013.
[2] R. Butler, A.T. Rhead, W. Liu and N. Kontis. Compressive strength of delaminated aerospace composites. *Phil. Trans. Roy. Soc. A*, Vol. 370: 1759-1779, 2012.
[3] G. W. Hunt, B. Hu, R. Butler, D. P. Almond, and J. E. Wright. Nonlinear modeling of delaminated struts. *AIAA Journal*, Vol. 42(11): 2364-2372, 2004.
[4] A.T. Rhead, R. Butler, G. Hunt. Post-buckled propagation model for compressive fatigue of impact damaged laminates. *Int. J. Sols. Struct.*, Vol. 45: 4349-4361, 2008.
[5] MATLAB R2013b, The MathWorks Inc., Natick, MA, 2013.
[6] S.J Winckler. Hygrothermally curvature stable laminates with tension-torsion coupling. *Journal of the American Helicopter Society*, Vol. 30 (3): 56-58, 1985.
[7] M. C.Y. Niu. Advanced Composite Structures. In M. C.Y. Niu, *Airframe Structural Design - Practical Design Information and Data on Aircraft Structures (2nd Edition)*, pages 511-516. Hong Kong: Conmilit Press Ltd., 1999.
[8] M.J. Shaurt. Failure of compression-loaded multidirectional composite laminates, *AIAA Journal*, Vol. 27(9): 1274-1279, 1989.